

2. Methods

2.1. BW removal algorithms

High-pass filtering (HPF), median filtering (MF), adaptive filtering (AF) and wavelet adaptive filtering (WAF) – which are common techniques for BW removal – and the recent approach based on QVR, are compared in this study. The high-pass filter is a linear-phase FIR filter synthesized applying the window method [14] using a Kaiser window, with 0.1 dB ripple in passband and 80 dB attenuation in stopband, and cut-off frequency 0.67 Hz compliant with AHA recommendations [4]. The window size of the median filter is chosen adapting the criterion proposed in [9] to the sampling frequency of 360 Hz. The convergence parameter of the adaptive filter [8] and the wavelet adaptive filter [11] is settled to obey AHA requirements on cut-off frequency [4]. The parameter λ of QVR [12] was set to 2×10^4 , without fine tuning.

2.2. ECG signals

ECG records from the MIT-BIH Arrhythmia Database [15] from PhysioNet [16] were considered. The database collects two-channel recordings acquired at a sampling frequency of 360 Hz with 11-bit resolution. In particular, the record mitdb/119 is from a 51 years old woman having frequent premature ventricular complexes (PVCs): about one beat over four is a PVC. We considered the first 5 minutes of the record, which are mostly free from BW, and corrupted them with different realizations of BW from the record nstdb/bw in the MIT-BIH Noise Stress Test Database [17] from PhysioNet [16]. This is a two-channel recording acquired at a sampling frequency of 360 Hz from a physically active volunteer, placing the electrodes on the limbs in positions in which the subject’s ECG was not visible [17].

Four non-overlapping realizations of BW, each 5 minutes long, were extracted from each channel of the recording nstdb/bw. Then, the eight realizations of baseline drift were added to the two BW free ECGs from record mitdb/119, thus obtaining sixteen ECGs with wandering. An example of BW free ECG and ECG affected by BW is reported in Figure 1 in panels a) and b), respectively.

The BW free records were manually segmented by an expert, by using PhysioNet manual annotations. ECG records have been partitioned into: PVCs, ST segments of normal beats, and normal beats excluding the ST segment. In total 247 ST segments and 80 PVCs were detected on the two BW free ECGs. Detected ectopic beats were checked to be consistent with those annotated in PhysioNet [16].

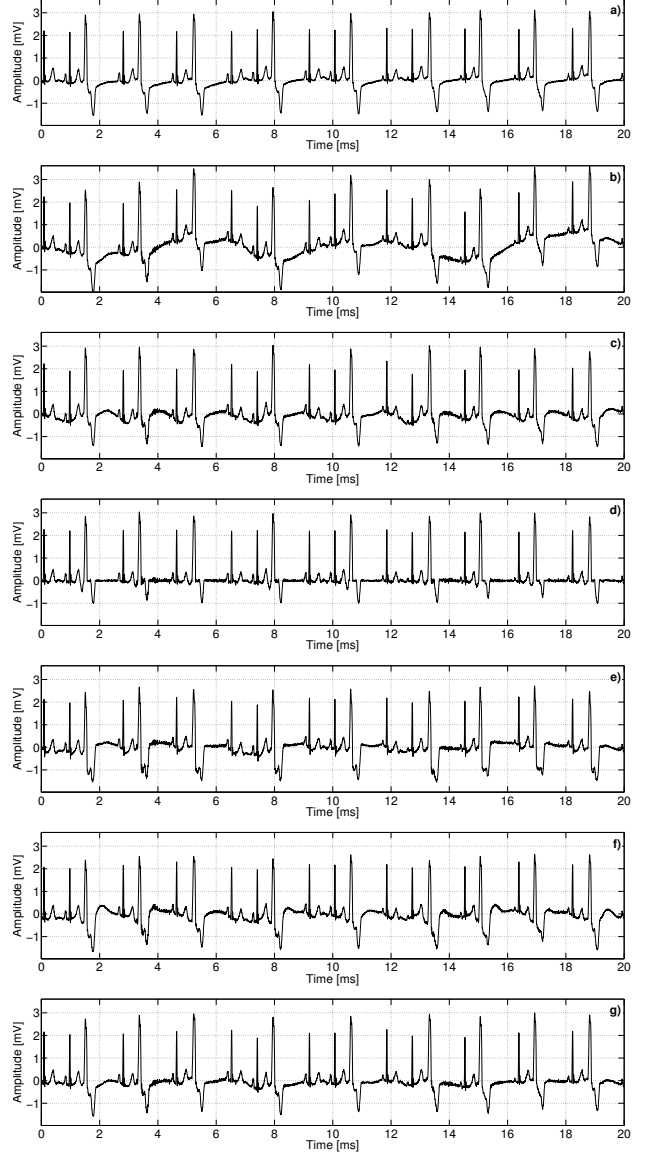


Figure 1. From top to bottom: a) portion of ECG record mitdb/119, which is BW free and exhibits some PVCs; b) the same record corrupted by BW from the record nstdb/bw; c)–g) records detrended using HPF, MF, AF, WAF, and QVR, respectively.

2.3. Performance metrics

The use of BW free ECGs corrupted with a priori known BW allows us to quantitatively assess the performance. The quality of BW removal is evaluated through the following quantity

$$\varepsilon [\tilde{\mathbf{b}}_i(\text{alg}_k), \mathbf{b}_i] = \frac{\|\tilde{\mathbf{b}}_i(\text{alg}_k) - \mathbf{b}_i\|^2}{\|\mathbf{b}_i\|^2} \quad (1)$$

	μ_ϵ	σ_ϵ	$\tilde{\epsilon}$	μ_ϵ^{ST}	$\sigma_\epsilon^{\text{ST}}$	$\tilde{\epsilon}^{\text{ST}}$	$\mu_\epsilon^{\text{PVC}}$	$\sigma_\epsilon^{\text{PVC}}$	$\tilde{\epsilon}^{\text{PVC}}$	$\mu_\epsilon^{\text{NB-ST}}$	$\sigma_\epsilon^{\text{NB-ST}}$	$\tilde{\epsilon}^{\text{NB-ST}}$
HPF	0.38	0.38	0.20	9.73	44.96	0.34	5.84	18.81	0.75	6.78	29.89	0.40
MF	0.68	0.70	0.35	6.66	28.84	0.38	16.87	45.06	2.95	3.72	14.75	0.32
AF	0.71	0.67	0.41	7.94	32.33	0.48	16.92	44.61	3.06	4.11	15.42	0.46
WAF	0.58	0.57	0.32	5.77	25.90	0.31	13.24	35.61	2.14	6.01	31.35	0.39
QVR	0.22	0.17	0.16	4.34	20.66	0.21	3.11	9.17	0.52	3.10	13.15	0.23

Table 1. Mean, standard deviation, and median of baseline estimation error (1) over: entire records ($\mu_\epsilon, \sigma_\epsilon, \tilde{\epsilon}$), ST segments ($\mu_\epsilon^{\text{ST}}, \sigma_\epsilon^{\text{ST}}, \tilde{\epsilon}^{\text{ST}}$), PVCs ($\mu_\epsilon^{\text{PVC}}, \sigma_\epsilon^{\text{PVC}}, \tilde{\epsilon}^{\text{PVC}}$), and normal beats excluding the ST segment ($\mu_\epsilon^{\text{NB-ST}}, \sigma_\epsilon^{\text{NB-ST}}, \tilde{\epsilon}^{\text{NB-ST}}$).

where \mathbf{b}_i denotes the generic BW realization, and $\tilde{\mathbf{b}}_i(\text{alg}_k)$ is the corresponding baseline estimated using the algorithm $\text{alg}_k \in \{\text{HPF}, \text{MF}, \text{AF}, \text{WAF}, \text{QVR}\}$. For each ECG with wandering, the (relative) estimation error (1) was computed on the entire record, and on *each* single PVC, ST segment, and normal beat excluding the ST segment. Estimation errors were computed over 16 ECGs with wandering, 1280 PVCs, 3936 ST segments, and 3936 normal beats excluding the ST segment, respectively.

Performance of different algorithms is measured in terms of the empirical distribution function of the corresponding errors (1), namely

$$\hat{F}(\epsilon) = \frac{1}{N} \sum_{i=1}^N \chi_{(-\infty, \epsilon]} \left(\epsilon \left[\tilde{\mathbf{b}}_i(\text{alg}_k), \mathbf{b}_i \right] \right) \quad (2)$$

where $\chi_{(-\infty, \epsilon]}$ denotes the indicator function of the set $(-\infty, \epsilon]$, and N is the number of generated baseline realizations. The use of the empirical distribution function is motivated by the fact that it provides a *complete* statistical description of the performance of each algorithm and allows us to compare algorithms over the *full range* of errors taking account of error relative frequencies. Moreover, some statistical indices are computed.

3. Numerical results

As an example, in Figure 1 we report a 20 s segment of the BW free ECG record (panel a)) corrupted by BW from the record nstdb/bw (panel b)). In panels from c) to g) we report the corresponding signals detrended using HPF, MF, AF, WAF, and QVR, respectively. Comparing them with the BW free record in panel a), the following considerations can be drawn. A residual drift is still present in the signal detrended by HPF, whereas MF (panel d)) introduces evident distortion in the detrended record. PVCs appear distorted in the records detrended by AF (panel e)) and WAF (panel f)). On the contrary, the panel corresponding to QVR (g)) shows that baseline drift has been removed, while the morphology of normal beats and PVCs has not been altered.

To quantitatively assess performance, we computed the baseline estimation error (1) considering: i) entire records,

ii) ST segments, iii) PVCs, and iv) normal beats excluding the ST segment (i.e., the remaining portions of the record). Figure 2 reports the empirical distribution functions of errors (1) for the BW removal algorithms under analysis, from top to bottom: ST segments (panel a)), PVCs (panel b)), and normal beats excluding the ST segment (panel c)). The empirical distribution function relative to the baseline estimation error on entire records is not reported since it consists of few points. As Figure 2 highlights, BW removal by QVR exhibits the best performance, since the corresponding empirical distribution function dominates the others. This implies that QVR exhibits lower errors with higher probability, thus introducing minor distortion in ECG signal morphology. Such behavior is maintained also for higher values of the error (not shown in the figure). Thus, QVR exhibits the best performance over the full range of errors.

This is also confirmed by the results of Table 1, where we report the mean, standard deviation, and median of baseline estimation error (1) computed for: i) entire records ($\mu_\epsilon, \sigma_\epsilon, \tilde{\epsilon}$ over 16 records); ii) ST segments ($\mu_\epsilon^{\text{ST}}, \sigma_\epsilon^{\text{ST}}, \tilde{\epsilon}^{\text{ST}}$ over 3936 ST segments); iii) PVCs ($\mu_\epsilon^{\text{PVC}}, \sigma_\epsilon^{\text{PVC}}, \tilde{\epsilon}^{\text{PVC}}$ over 1280 ectopic beats); iv) normal beats excluding the ST segment ($\mu_\epsilon^{\text{NB-ST}}, \sigma_\epsilon^{\text{NB-ST}}, \tilde{\epsilon}^{\text{NB-ST}}$ over 3936 normal beats).

As Table 1 and Figure 2 highlight, QVR outperforms state-of-the-art algorithms in estimating BW, while preserving the morphology of all waveforms in ECG, both in normal and ectopic beats. It is worth remarking that the median, which is a more robust index of centrality [18], is significantly lower for QVR than competing algorithms.

4. Conclusions

In this paper we assessed the impact of different BW removal techniques on ECG signal morphology. The methods considered were: high-pass filtering, median filtering, adaptive filtering, wavelet adaptive filtering, and our recent approach based on QVR. BW free ECGs, exhibiting normal and ectopic beats, were corrupted with different realizations of known BW. The baseline estimation error was computed to quantify both the effectiveness in removing BW and the distortion introduced in beat morphol-

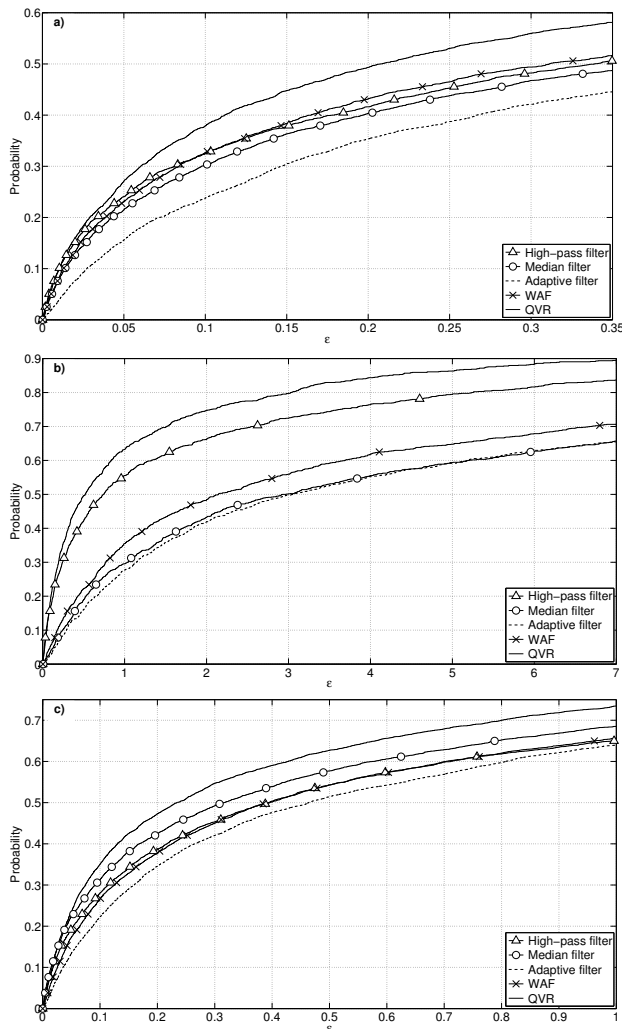


Figure 2. Empirical distribution functions of baseline estimation error (1) computed on: a) ST segments, b) PVCs, and c) normal beats excluding the ST segment.

ogy. Numerical results show that the approach based on QVR outperforms state-of-the-art algorithms in estimating BW, while preserving the morphology of all waveforms in ECG, both in normal and ectopic beats.

References

- [1] Sörnmo L, Laguna P. *Bioelectrical Signal Processing in Cardiac and Neurological Applications*. Elsevier Academic Press, 2005.
- [2] Malmivuo J, Plonsey R. *Bioelectromagnetism - Principles and Applications of Bioelectric and Biomagnetic Fields*. Oxford University Press, 1995.
- [3] Clifford GD, Azuaje F, McSharry P (eds.). *Advanced Methods and Tools for ECG Data Analysis*. Artech House, Inc., 2006.
- [4] Kligfield P, Gettes LS, Bailey JJ, Childers R, Deal BJ, Hancock EW, van Herpen G, Kors JA, Macfarlane P, Mirvis DM, Pahlm O, Rautaharju P, Wagner GS. Recommendations for the standardization and interpretation of the electrocardiogram: Part I: The electrocardiogram and its technology. *Circulation* 2007;115:1306–1324.
- [5] Califf RM, Roe MT. *ACS Essentials*. Jones and Bartlett Publishers, 2010.
- [6] Brewer AJ, Lane ES, Ross P, Hachwa B. Misdiagnosis of perioperative myocardial ischemia: The effects of electrocardiogram filtering. *Anesth Analg* 2006;103(6):1632–1634.
- [7] Van Alsté JA, Schilder TS. Removal of base-line wander and power-line interference from the ECG by an efficient FIR filter with a reduced number of taps. *IEEE Trans Biomed Eng* 1985;32(12):1052–1060.
- [8] Thakor NV, Zhu YS. Applications of adaptive filtering to ECG analysis: Noise cancellation and arrhythmia detection. *IEEE Trans Biomed Eng* 1991;38(8):785–794.
- [9] Hiasat AA, Al-Ibrahim MM, Gharaibeh KM. Design and implementation of a new efficient median filtering algorithm. *IEE Proc Vis Image Signal Process* 1999;146(5):273–278.
- [10] Meyer CR, Keiser HN. Electrocardiogram baseline noise estimation and removal using cubic splines and state-space computation techniques. *Comp Biomed Res* 1977;10(5):459–470.
- [11] Park KL, Lee KJ, Yoon HR. Application of a wavelet adaptive filter to minimise distortion of the ST-segment. *Med Biol Eng Comp* 1998;36(5):581–586.
- [12] Fasano A, Villani V, Vollerio L. Baseline wander estimation and removal by quadratic variation reduction. *Proc 33rd Int Conf IEEE Eng Med Biol Soc EMBC* 2011;977–980.
- [13] Fasano A, Villani V, Vollerio L. Fast ECG baseline wander removal preserving the ST segment. *Proc 4th Int Symp Appl Sci Biomed Commun Tech ISABEL* 2011;.
- [14] Oppenheim AV, Schaffer RW, Buck JR. *Discrete-Time Signal Processing*. 2nd edition. Prentice-Hall, Inc., 1999.
- [15] Moody GB, Mark RG. The impact of the MIT-BIH arrhythmia database. *IEEE Trans Biomed Eng* 2001;20(3):45–50.
- [16] Goldberger AL, Amaral LAN, Glass L, Hausdorff JM, Ivanov PC, Mark RG, Mietus JE, Moody GB, Peng CK, Stanley HE. *PhysioBank, PhysioToolkit, and PhysioNet: Components of a new research resource for complex physiologic signals*. *Circulation* 2000;101(23):e215–e220.
- [17] Moody GB, Muldrow W, Mark RG. A noise stress test for arrhythmia detectors. *Computers in Cardiology* 1984;11:381–384.
- [18] Huber PJ, Ronchetti EM. *Robust Statistics*. Wiley, 2009.

Address for correspondence:

Antonio Fasano
 Università Campus Bio-Medico di Roma
 via Álvaro del Portillo, 21
 00128 Rome, Italy
 E-mail: a.fasano@unicampus.it